Transactions of the Nigerian Association of Mathematical Physics
Volume 1, (November, 2015), **pp 21 – 32**

Single Hole Dynamics in One Dimensional Quantum Antiferromagnet.

S. Ehika[1] and J.O.A. Idiodi[2]

[1]Department of physics, Ambrose Alli University, Ekpoma, Edo State, Nigeria.
[2]Department of Physics, University of Benin, Benin City, Nigeria.

Abstract

Exact diagonalization (ED) study on 1D cuprates doped with a single hole and modelled by the more realistic $t-J$ Hamiltonian is carried out on finite one dimensional systems up to eight sites. The energy expended by the hole is found to decrease with the system size. This observation is in contrast to the motion of a hole in Ising antiferromagnetic chain, where the hole energy increases slightly with system size. This lowering of the energy of the hole gives a coherent propagation to the hole, at least in the weak coupling regime $(J<<1)$. Evidently, this reduction in the energy of the hole is due to the quantum spin fluctuation term in the $t-J$ model that helps to "heal" pair of flipped spins created by hole dynamics. In the strong coupling regime, the energy of the hole is positive at $J=0.8$ and $J=1.0$ for four and eight sites respectively. Hence, in this regime, the hole shows more tendencies to be confined for shorter lengths than longer lengths of propagation. This is an exact opposite to what is observed for the case of the Ising model, and is also in stark contrast to the behaviour of a hole in two dimensional antiferromagnet, where confinement grows with the distance travelled by the hole. This deconfinement of hole in one dimensional quantum antiferromagnet lends credence to both theoretical and experimental reports of spin charge separation in one dimensional Mott Insulator.

Keywords: Quantum antiferromagnet, hole confinement, thermodynamic limit, exact diagonalization and spin-charge separation.

1.0 Introduction

The discovery of high temperature superconductors (HTSC) in oxides of copper [1] has stimulated great interest in the studies of the interplay between magnetism and superconductivity. It has already been established that the reference compounds like La_2CuO_4 in the case of lanthanum family or Y $Ba_2Cu_3O_6$ for the yttrium family are antiferromagnetic (AF) Mott insulators [2]. Upon doping, the AF long range order fades away and superconductivity occurs below certain critical temperature. It is generally believed that a comprehensive understanding of the doping evolution from Mott insulator to superconductor holds the key to the mystery of HTSC. This belief has led to the experimental and theoretical study of the dynamics of one or more holes in two dimensional (2D) antiferromagnets. A theoretical study of the dynamics of one hole in 2D AF, for instance, is the well known spin polaron (SP) approach, which is based on the physical mechanism that hole motion in the AF gives rise to the creation of spin fluctuations [3-5]. The conclusion drawn from this approach, which has been confirmed experimentally, is the formation of four hole pockets located around points $(\pm\pi/2,\pm\pi/2)$ [6-7]. However, researchers are yet to reach concrete consensus as regards the robustness of the $t-J$ model to capture the mechanism of superconductivity in the cuprates [8-11].

There have also been rigorous and intense researches on one dimensional (1D) Mott insulators. The motivation for researches on these insulators is because of the intriguing phenomena that have been discovered theoretically and experimentally in them. For instance, it has been reported both theoretically and experimentally that spin and charge degrees of freedom are

Corresponding author: S. Ehika, E-mail: ehikasimon@yahoo.com, Tel.: +2348074478911

separated in the 1D correlated electron systems, and behave as independent elementary excitations called ‘‘spinon’’ and ‘‘holon’’, respectively [12-18]. More so, an experiment with Sr_2CuO_3, which is a one 1D Mott insulator, found an orbiton liberating itself from spinons and propagating through the lattice as a distinct quasi-particle with a substantial dispersion of ~ 0.2eV [19]. This observation of a free orbiton is another example of particle fractionalization known as Spin-orbital separation. In ref. [20], further fractionalization of spin and charge beyond the Luttinger-liguid paradigm was discovered. These reviews point out the relevance of 1D and quasi 1D cuprates in the scheme of magnetism and high-T_c superconductors. This field of strongly correlated electron systems is still embryonic and lots of theoretical and experimental researches are geared towards addressing some of the problems associated with hole(s) dynamics. The aim of the present work is to study the dynamics of a single hole in one dimensional quantum antiferromagnet, using the more realistic $t-J$ model, and with the aid of exact diagonalization (ED) method. It is hoped that this theoretical study will shed more light on some elusive aspect of hole dynamics and provide further evidence of spinon-holon decoupling in the thermodynamic limit. The rest of the paper is organized as follows: In section 2, the $t-J$ model in 1D and the effective Hamiltonian describing the hole dynamics in the presence of quantum spin fluctuations are presented. Section 3 provides the Hilbert arising from both hole and spin dynamics In section 4, we carry out exact diagonalization of some finite chains. In section 5, we present and discuss the numerical ground state energy of the hole as a function of the coupling parameter J. A brief conclusion will close the paper in section 6.

2.0 The Generalized *t-J* Model

Experimental results have suggested that the Hubbard models (one-and two-band) [21], where electrons interact through an on-site Coulombic repulsion (U) should be analysed in the strong coupling region ($U/t >> 1$). In this strong coupling limit, the one-band Hubbard model can be mapped into an effective $t-J$ model. This Hamiltonian is given by

$$H = -t\sum_{\langle i,j\rangle\sigma}\left(\tilde{c}^{+}_{i\sigma}\tilde{c}_{i\sigma} + \tilde{c}^{+}_{J\sigma}\tilde{c}_{i\sigma}\right) + J\sum_{\langle i,j\rangle\sigma}\left[S_i^z\cdot S_j^z + \frac{J}{2}\left(S_i^+S_j^- + S_i^-S_j^+\right)\right], \quad (1)$$

with the spin operators defined in the usual second quantized form as

$$\left.\begin{aligned} S_i^z &= \frac{1}{2}\left(c^{\dagger}_{i\uparrow}c_{i\uparrow} - c^{\dagger}_{i\downarrow}c_{i\downarrow}\right)\\ S_i^+ &= c^{\dagger}_{i\uparrow}c_{i\downarrow}\\ S_i^- &= c^{\dagger}_{i\downarrow}c_{i\uparrow}\end{aligned}\right\}. \quad (2)$$

Here, $\langle i,j\rangle$ implies that interactions are restricted to nearest neighbour, and $\tilde{c}^{\dagger}_{i\sigma}$ ($\tilde{c}_{i\sigma}$) is the creation (annihilation) operator of an electron with spin σ at the lattice site i, in a space where double occupancy is forbidden, i.e.

$$\tilde{c}^{\dagger}_{i\sigma} = c^{\dagger}_{i\sigma}(1-n_{i.-\sigma}). \quad (3)$$

In this derivation of the $t-J$ Hamiltonian, the hoping integral t and the exchange constant J are connected by

$$J = 4t^2/U. \quad (4)$$

The effective hole Hamiltonian is given by

$$H' = H - H_{Hen}. \quad (5)$$

Here, H_{Hen} is the Heisenberg Hamiltonian of the half-filled system without a hole, diagonalized in the subspace of $S^z_{tot} = 0$. The energy of a single hole relative to the Neél background is given by

$$\in_h = \in_t - \in_N, \quad (6)$$

where $\in_t$ is the ground state energy of the Hamiltonia in (1) and $\in_N$ is the ground state energy of the isotropic antiferromagnetic Heisenberg chain. The exact mapping from Hubbard model to $t-J$ model also includes a three site term, which is neglected here because it is believed not to change the physics of the model, at least in one dimension.

3.0 Hilbert Space of a Single Hole In The *t-J* Model

It has been established that the undoped cuprates display conventional Neel order which can be described by quantum Heisenberg model. When doped, the long-range antiferromagnetic order is destroyed and superconductivity appears. This disappearance of antiferromagnetic ordering shows that the carries (holes) are not static but mobile. The central issue is to see how the spin flip term in the $t-J$ influences the dynamics of a single hole.

In this model, even chains subject to periodic boundary conditions (PBC) are considered. At half filling, the ground state is antiferromagnetic (i.e $|\mathrm{N}\rangle = |\downarrow,\uparrow,\downarrow,\cdots\rangle$). Out of the two states obtained by translation of one lattice vector, the one with a spin down at the origin is selected. The annihilation of the spin down electron at the origin defines the starting state, i.e. $|0\rangle = c_{0\downarrow}|N\rangle$. New states are generated by the action of spin flip term as well as the action of hole hoping term. The size of the Hilbert space spanned by the action of the hoping term in the $t-J$ model is given by

$$S_{hole} = N(N-1), \tag{7}$$

where N is the number of sites. The size of the space generated by the quantum spin fluctuation term is given by

$$S_{flip} = N - N^2 + \frac{2(N-1)!}{\left[\left(\frac{N-2}{2}\right)!\right]^2}. \tag{8}$$

Hence, the total state due to hole and spin dynamics is given by

$$S_{tot} = \frac{2(N-1)!}{\left[\left(\frac{N-2}{2}\right)!\right]^2}. \tag{9}$$

The new states generated when the kinetic part of (1) acts on the states in (7) are orthogonal to the state in (8). Hence, the subspace in (7), under the action of the kinetic term, is self-contained. The translational invariance property of the $t-J$ model will be utilized in reducing the size of the Hilbert space of a single hole. This means that any one hole state with definite momentum k and spin ↑ can be written as

$$|\psi_k\rangle = \frac{1}{\sqrt{L}}\sum_{R=0}^{L-1} e^{-ikR} T_L^R c_{0\downarrow}|\sigma_0\rangle, \tag{10}$$

where $|\sigma_0\rangle$ is a suitable spin state with the spin at the origin $R=0$ fixed to ↓, and T_L is the spin translation operator defined by the transformation property

$$T_L S_R T_L^{-1} = S_{R+1}, \tag{11}$$

where periodic boundary conditions (PBC) over the L sites are assumed in order to define the effect of translation at the rightmost site. With translational symmetry, the size of the Hilbert space is reduced by a factor of N according to the equation

$$S_{tot} = \frac{2(N-1)!}{N\left[\left(\frac{N-2}{2}\right)!\right]^2}. \tag{12}$$

4.0 Exact Diagonalization of Finite Chains

In this section, exact diagonalization of some finite systems with PBC will be implemented.

4.1 Four Sites Chain

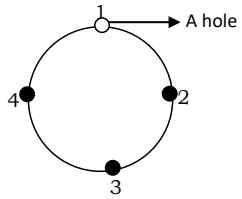

Fig.1: A four sites chain with a hole subject to periodic boundary conditions.

The Neél states of this system obtained by translation of one lattice vector are $|1\uparrow,2\downarrow 3\uparrow,4\downarrow\rangle$ and $|1\downarrow 2\uparrow,3\downarrow,4\uparrow\rangle$.

Since we are interested in the subspace of $S_{tot}^z = 1/2$, the annihilation of say the down spin electron at site 1 defines our

starting state. This state denoted by $|0\rangle$ is given by $|0\rangle = |1,2\uparrow,3\downarrow,4\uparrow\rangle$. Due to the small size of this system, the Hilbert space can be provided by either the action of the kinetic part or by the action of the quantum spin fluctuation term in (1). By implementing the translational symmetry discussed in section 3, the Hilbert space of this system of size 12 is reduced to 3 according to (10), using (12). These normalized states are listed below.

$$|\phi_0\rangle = \frac{1}{2}\left[|1,2\uparrow,3\downarrow,4\uparrow\rangle + |1\uparrow,2,3\uparrow,4\downarrow\rangle + |1\downarrow,2\uparrow,3,4\uparrow\rangle + |1\uparrow,2\downarrow,3\uparrow,4\rangle\right]$$

$$|\phi_1\rangle = \frac{1}{2}\left[|1,2\downarrow,3\uparrow,4\uparrow\rangle + |1\uparrow,2,3\downarrow,4\uparrow\rangle + |1\uparrow,2\uparrow,3,4\downarrow\rangle + |1\downarrow,2\uparrow,3\uparrow,4\rangle\right]$$

$$|\phi_2\rangle = \frac{1}{2}\left[|1,2\uparrow,3\uparrow,4\downarrow\rangle + |1\downarrow,2,3\uparrow,4\uparrow\rangle + |1\uparrow,2\downarrow,3,4\uparrow\rangle + |1\uparrow,2\uparrow,3\downarrow,4\rangle\right]$$

Application of H to these states gives

$$H|\phi_0\rangle = -t|\phi_1\rangle - t|\phi_2\rangle - \frac{J}{2}|\phi_0\rangle + \frac{J}{2}|\phi_1\rangle + \frac{J}{2}|\phi_2\rangle$$

$$H|\phi_1\rangle = -t|\phi_0\rangle - t|\phi_2\rangle + \frac{J}{2}|\phi_0\rangle$$

$$H|\phi_2\rangle = -t|\phi_0\rangle - t|\phi_1\rangle + \frac{J}{2}|\phi_0\rangle$$

The Hamiltonian matrix for these operations is

$$H = \begin{bmatrix} -\frac{J}{2} & -t+\frac{J}{2} & -t+\frac{J}{2} \\ \frac{J}{2}-t & 0 & -t \\ \frac{J}{2}-t & -t & 0 \end{bmatrix}. \tag{13}$$

The ground state energy of this matrix is

$$\in_t = 1/2(J-4t). \tag{14}$$

The variation of this ground state energy with J at $t=1$ is presented in section 5.

4.2 Six Sites Chain

By using translational symmetry, taking into account the states generated by both the hole hoping and quantum spin fluctuations, the normalized state for the six sites chain are:

$$|\phi_0\rangle = \frac{1}{\sqrt{6}}\left[\begin{array}{l} |1,2\uparrow,3\downarrow,4\uparrow,5\downarrow,6\uparrow\rangle + |1\uparrow,2,3\uparrow,4\downarrow,5\uparrow,6\downarrow\rangle + |1\downarrow,2\uparrow,3,4\uparrow,5\downarrow,6\uparrow\rangle \\ + |1\uparrow,2\downarrow,3\uparrow,4,5\uparrow,6\downarrow\rangle + |1\downarrow,2\uparrow,3\downarrow,4\uparrow,5,6\uparrow\rangle + |1\uparrow,2\downarrow,3\uparrow,4\downarrow,5\uparrow,6\rangle \end{array}\right]$$

$$|\phi_1\rangle = \frac{1}{\sqrt{6}}\left[\begin{array}{l} |1,2\downarrow,3\uparrow,4\downarrow,5\uparrow,6\uparrow\rangle + |1\uparrow,2,3\downarrow,4\uparrow,5\downarrow,6\uparrow\rangle + |1\uparrow,2\uparrow,3,4\downarrow,5\uparrow,6\downarrow\rangle \\ + |1\downarrow,2\uparrow,3\uparrow,4,5\downarrow,6\uparrow\rangle + |1\uparrow,2\downarrow,3\uparrow,4\uparrow,5,6\downarrow\rangle + |1\downarrow,2\uparrow,3\downarrow,4\uparrow,5\uparrow,6\rangle \end{array}\right]$$

$$|\phi_2\rangle = \frac{1}{\sqrt{6}}\left[\begin{array}{l} |1,2\uparrow,3\uparrow,4\downarrow,5\uparrow,6\downarrow\rangle + |1\downarrow,2,3\uparrow,4\uparrow,5\downarrow,6\uparrow\rangle + |1\uparrow,2\downarrow,3,4\uparrow,5\uparrow,6\downarrow\rangle \\ + |1\downarrow,2\uparrow,3\downarrow,4,5\uparrow,6\uparrow\rangle + |1\uparrow,2\downarrow,3\uparrow,4\downarrow,5,6\uparrow\rangle + |1\uparrow,2\uparrow,3\downarrow,4\uparrow,5\downarrow,6\rangle \end{array}\right]$$

$$|\phi_3\rangle = \frac{1}{\sqrt{6}}\left[\begin{array}{l} +|1,2\uparrow,3\downarrow,4\uparrow,5\uparrow,6\downarrow\rangle + |1\downarrow,2,3\uparrow,4\downarrow,5\uparrow,6\uparrow\rangle + |1\uparrow,2\downarrow,3,4\uparrow,5\downarrow,6\uparrow\rangle \\ + |1\uparrow,2\uparrow,3\downarrow,4,5\uparrow,6\downarrow\rangle + |1\downarrow,2\uparrow,3\uparrow,4\downarrow,5,6\uparrow\rangle + |1\uparrow,2\downarrow,3\uparrow,4\uparrow,5\downarrow,6\rangle \end{array}\right]$$

$$|\phi_4\rangle = \frac{1}{\sqrt{6}}\left[\begin{array}{l} |1,2\downarrow,3\uparrow,4\uparrow,5\downarrow,6\uparrow\rangle + |1\uparrow,2,3\downarrow,4\uparrow,5\uparrow,6\downarrow\rangle + |1\downarrow,2\uparrow,3,4\downarrow,5\uparrow,6\uparrow\rangle \\ + |1\uparrow,2\downarrow,3\uparrow,4,5\downarrow,6\uparrow\rangle + |1\uparrow,2\uparrow,3\downarrow,4\uparrow,5,6\downarrow\rangle + |1\downarrow,2\uparrow,3\uparrow,4\downarrow,5\uparrow,6\rangle \end{array}\right]$$

$$|\phi_5\rangle = \frac{1}{\sqrt{6}}\left[\begin{array}{l} |1,2\uparrow,3\uparrow,4\downarrow,5\downarrow,6\uparrow\rangle + |1\uparrow,2,3\uparrow,4\uparrow,5\downarrow,6\downarrow\rangle + |1\downarrow,2\uparrow,3,4\uparrow,5\uparrow,6\downarrow\rangle \\ + |1\downarrow,2\downarrow,3\uparrow,4,5\uparrow,6\uparrow\rangle + |1\uparrow,2\downarrow,3\downarrow,4\uparrow,5,6\uparrow\rangle + |1\uparrow,2\uparrow,3\downarrow,4\downarrow,5\uparrow,6\rangle \end{array}\right]$$

$$|\phi_6\rangle = \frac{1}{\sqrt{6}}\left[\begin{array}{l}|1,2\uparrow,3\downarrow,4\downarrow,5\uparrow,6\uparrow\rangle + |1\uparrow,2,3\uparrow,4\downarrow,5\downarrow,6\uparrow\rangle + |1\uparrow,2\uparrow,3,4\uparrow,5\downarrow,6\downarrow\rangle \\ + |1\downarrow,2\uparrow,3\uparrow,4,5\uparrow,6\downarrow\rangle + |1\downarrow,2\downarrow,3\uparrow,4\uparrow,5,6\uparrow\rangle + |1\uparrow,2\downarrow,3\downarrow,4\uparrow,5\uparrow,6\rangle\end{array}\right]$$

$$|\phi_7\rangle = \frac{1}{\sqrt{6}}\left[\begin{array}{l}|1,2\downarrow,3\uparrow,4\uparrow,5\uparrow,6\downarrow\rangle + |1\downarrow,2,3\downarrow,4\uparrow,5\uparrow,6\uparrow\rangle + |1\uparrow,2\downarrow,3,4\downarrow,5\uparrow,6\uparrow\rangle \\ + |1\uparrow,2\uparrow,3\downarrow,4,5\downarrow,6\uparrow\rangle + |1\uparrow,2\uparrow,3\uparrow,4\downarrow,5,6\downarrow\rangle + |1\downarrow,2\uparrow,3\uparrow,4\uparrow,5\downarrow,6\rangle\end{array}\right]$$

$$|\phi_8\rangle = \frac{1}{\sqrt{6}}\left[\begin{array}{l}|1,2\uparrow,3\uparrow,4\uparrow,5\downarrow,6\downarrow\rangle + |1\downarrow,2,3\uparrow,4\uparrow,5\uparrow,6\downarrow\rangle + |1\downarrow,2\downarrow,3,4\uparrow,5\uparrow,6\uparrow\rangle \\ + |1\uparrow,2\downarrow,3\downarrow,4,5\uparrow,6\uparrow\rangle + |1\uparrow,2\uparrow,3\downarrow,4\downarrow,5,6\uparrow\rangle + |1\uparrow,2\uparrow,3\uparrow,4\downarrow,5\downarrow,6\rangle\end{array}\right]$$

$$|\phi_9\rangle = \frac{1}{\sqrt{6}}\left[\begin{array}{l}|1,2\downarrow,3\downarrow,4\uparrow,5\uparrow,6\uparrow\rangle + |1\uparrow,2,3\downarrow,4\downarrow,5\uparrow,6\uparrow\rangle + |1\uparrow,2\uparrow,3,4\downarrow,5\downarrow,6\uparrow\rangle \\ + |1\uparrow,2\uparrow,3\uparrow,4,5\downarrow,6\downarrow\rangle + |1\downarrow,2\uparrow,3\uparrow,4\uparrow,5,6\downarrow\rangle + |1\downarrow,2\downarrow,3\uparrow,4\uparrow,5\uparrow,6\rangle\end{array}\right]$$

The action of H on the reduced Hilbert space, gives

$$H|\phi_0\rangle = -t|\phi_1\rangle - t|\phi_2\rangle - J|\phi_0\rangle + \frac{J}{2}|\phi_3\rangle + \frac{J}{2}|\phi_4\rangle + + \frac{J}{2}|\phi_5\rangle + \frac{J}{2}|\phi_6\rangle$$

$$H|\phi_1\rangle = -t|\phi_0\rangle - t|\phi_3\rangle - \frac{J}{2}|\phi_1\rangle + \frac{J}{2}|\phi_4\rangle + \frac{J}{2}|\phi_6\rangle + \frac{J}{2}|\phi_9\rangle$$

$$H|\phi_2\rangle = -t|\phi_0\rangle - t|\phi_4\rangle - \frac{J}{2}|\phi_2\rangle + \frac{J}{2}|\phi_3\rangle + \frac{J}{2}|\phi_5\rangle + \frac{J}{2}|\phi_8\rangle$$

$$H|\phi_3\rangle = -t|\phi_1\rangle - t|\phi_4\rangle - \frac{J}{2}|\phi_3\rangle + \frac{J}{2}|\phi_0\rangle + \frac{J}{2}|\phi_2\rangle + \frac{J}{2}|\phi_7\rangle$$

$$H|\phi_4\rangle = -t|\phi_2\rangle - t|\phi_3\rangle - \frac{J}{2}|\phi_4\rangle + \frac{J}{2}|\phi_0\rangle + \frac{J}{2}|\phi_1\rangle + \frac{J}{2}|\phi_7\rangle$$

$$H|\phi_5\rangle = -t|\phi_6\rangle - t|\phi_8\rangle + \frac{J}{2}|\phi_0\rangle + \frac{J}{2}|\phi_2\rangle$$

$$H|\phi_6\rangle = -t|\phi_5\rangle - t|\phi_9\rangle + \frac{J}{2}|\phi_0\rangle + \frac{J}{2}|\phi_1\rangle$$

$$H|\phi_7\rangle = -t|\phi_9\rangle - t|\phi_8\rangle + \frac{J}{2}|\phi_3\rangle + \frac{J}{2}|\phi_4\rangle$$

$$H|\phi_8\rangle = -t|\phi_7\rangle - t|\phi_5\rangle + \frac{J}{2}|\phi_8\rangle + \frac{J}{2}|\phi_2\rangle$$

$$H|\phi_9\rangle = -t|\phi_7\rangle - t|\phi_6\rangle + \frac{J}{2}|\phi_9\rangle + \frac{J}{2}|\phi_1\rangle$$

The Hamiltonian matrix of these operations is

$$H = \begin{bmatrix} -J & -t & -t & \frac{J}{2} & \frac{J}{2} & \frac{J}{2} & \frac{J}{2} & 0 & 0 & 0 \\ -t & -\frac{J}{2} & 0 & -t & \frac{J}{2} & 0 & \frac{J}{2} & 0 & 0 & \frac{J}{2} \\ -t & 0 & -\frac{J}{2} & \frac{J}{2} & -t & \frac{J}{2} & 0 & 0 & \frac{J}{2} & 0 \\ \frac{J}{2} & -t & \frac{J}{2} & -\frac{J}{2} & -t & 0 & 0 & \frac{J}{2} & 0 & 0 \\ \frac{J}{2} & \frac{J}{2} & -t & -t & \frac{J}{2} & 0 & 0 & \frac{J}{2} & 0 & 0 \\ \frac{J}{2} & 0 & \frac{J}{2} & 0 & 0 & 0 & -t & 0 & -t & 0 \\ \frac{J}{2} & \frac{J}{2} & 0 & 0 & 0 & -t & 0 & 0 & 0 & -t \\ 0 & 0 & 0 & \frac{J}{2} & \frac{J}{2} & 0 & 0 & 0 & -t & -t \\ 0 & 0 & \frac{J}{2} & 0 & 0 & -t & 0 & -t & \frac{J}{2} & 0 \\ 0 & \frac{J}{2} & 0 & 0 & 0 & 0 & -t & -t & 0 & \frac{J}{2} \end{bmatrix} \qquad (15)$$

The ground state energy of this system at $t = J = 1$ is

$$E_g = -2.87559 . \quad (16)$$

The variation of the ground state energy with J at $t = 1$ is presented in section 5.

4.3 Eight -Site Chain

The size of the Hilbert space of this system in the subspace of $S^z_{tot} = 1/2$ is given by

$$N_h = \frac{2(N-1)!}{[(N/2-1)!]^2} = \frac{2\times 7!}{(3!)^2} = 280$$

The Hilbert space can drastically be reduced to 35 according to (10). The annihilation of the spin down electron at the origin defines the starting state, i.e.

$$|0\rangle = c_{1\downarrow}|1\downarrow,2\uparrow,3\downarrow,4\uparrow,5\downarrow,6\uparrow,7\downarrow,8\uparrow\rangle = |1,2\uparrow,3\downarrow,4\uparrow,5\downarrow,6\uparrow,7\downarrow,8\uparrow\rangle \quad (17)$$

The action of the translational operator in (10) on (17) gives

$$|\phi_0\rangle = \frac{1}{\sqrt{8}}\begin{bmatrix} |1,2\uparrow,3\downarrow,4\uparrow,5\downarrow,6\uparrow,7\downarrow,8\uparrow\rangle + |1\uparrow,2,3\uparrow,4\downarrow,5\uparrow,6\downarrow,7\uparrow,8\downarrow\rangle \\ +|1\downarrow,2\uparrow,3,4\uparrow,5\downarrow,6\uparrow,7\downarrow,8\uparrow\rangle + |1\uparrow,2\downarrow,3\uparrow,4,5\uparrow,6\downarrow,7\uparrow,8\downarrow\rangle \\ +|1\downarrow,2\uparrow,3\downarrow,4\uparrow,5,6\uparrow,7\downarrow,8\uparrow\rangle + |1\uparrow,2\downarrow,3\uparrow,4\downarrow,5\uparrow,6,7\uparrow,8\downarrow\rangle \\ +|1\downarrow,2\uparrow,3\downarrow,4\uparrow,5\downarrow,6\uparrow,7,8\uparrow\rangle + |1\uparrow,2\downarrow,3\uparrow,4\downarrow,5\uparrow,6\downarrow,7\uparrow,8\rangle \end{bmatrix} \quad (18)$$

The rest of the normalized states can be obtained from (18) by using both the kinetic and the spin flip term in (1). Unfortunately, in order to reduce the number of pages, these states are not shown in this work. However, they will readily be provided on demand. The ground state energy of this system at $t = J = 1$ is

$$\in_t = -3.38765 \quad (19)$$

The variation of the ground state energy with J at $t = 1$ is presented in section 5

5. 0 Numerical Result for Single Hole Energy In 1D

This section presents the numerical exact result for the energy of a single hole for 4, 6 and 8 sites at $t = 1$, as shown in Table 1, 2 and 3 respectively. From these Tables, it is observed that at $J = 0$ the energy of the hole is $\in_h = -2$. At this energy, the hole propagates freely through the antiferromagnetic background, since no magnetic energy cost is incurred. The energy expended by the hole is found to decrease slightly with the system size. This lowering of the energy of the hole gives a coherent propagation to the hole, at least in the weak coupling regime $(J << 1)$. Evidently, this reduction in the energy of the hole is due to the quantum spin fluctuation term in the $t - J$ model that helps to "heal" pair of flipped spins created by hole dynamics. This also means that the relaxation time for a pair of flipped spin is relatively short, so that the hole does not feel the presence of the spinon created as a result of its motion. In the strong coupling regime $(J >> 1)$, the motion of the hole is compromised because of the increase in magnetic energy cost. For instance, the energy of the hole for four sites is positive at $J = 0.8$ and positive at $J = 1$ for eight sites, as shown in Tables 1 and 3 respectively. Hence, the hole shows more tendencies to be confined for shorter lengths than longer lengths of propagation. This inverse relation between $\in_h$ and N as observed between four and eight sites is not quite obvious between six and eight sites. This might be due to the fact that the ground state energies of $N = 6$ and $N = 8$ do not belong to the same momentum space. It is known that the ground state energies of the half-filled Heisenberg even chains have momenta $k = 0$ and $k = \pi$ for $N = 4n$ and $N = 4n + 2$ respectively, where $n = 1,2,3,\cdots$. Hence, this trend should be expected either between $N = 8$ and $N = 12$ or between $N = 6$ and $N = 10$, that have ground state energies with momenta corresponding to $k = 0$ and $k = \pi$ respectively.
For the purpose of comparison, the exact result for a hole in one dimensional Ising antiferromagnet for four, six and eight sites is here reproduced in Tables 4, 5 and 6 respectively [22]. As seen from these Tables, weak confinement that vanishes at large N characterises the Ising chain. This obvious difference between the Ising chains and Heisenberg chains is due to the fact that the vanishing spinon in the former is dependent on the distant travelled (which is also proportional to N), while in the latter, it is dependent on both N and the spin flip term.

Table 1: The energy of one hole ($\in_h$) as a function of J for 4 sites

J	$\in_t$	$\in_N$	$\in_h$
0.000	-2.000	0.000	-2.000
0.010	-1.995	-0,020	-1.975
0.020	-1.990	-0.040	-1.950
0.050	-1.975	-0.100	-1.875
0.100	-1.950	-0.20	-1.750
0.200	-1.900	-0.400	-1.500
0.400	-1.800	-0.800	-1.000
0.600	-1.700	-1.200	-0.500
0.800	-1.600	-1.600	0.000
1.000	-1.500	-2.000	0.500
1.500	-1.250	-3.000	1.750
2.000	-1.000	-4.000	3.000
2.500	-1.500	-5.000	3.500
3.000	-2.000	-6.000	4.000
4.000	-3.000	-8.000	5.000

Table 2: The energy of one hole ($\in_h$) as a function of J for 6 sites

J	$\in_t$	$\in_N$	$\in_h$
0.00000	-2.00000	0.00000	-2.00000
0.01000	-2.00601	-0.02803	-1.97798
0.02000	-2.01205	-0.05601	-1.95604
0.05000	-2.03031	-0.14014	-1.89017
0.10000	-2.06121	-0.28028	-1.78093
0.20000	-2.12532	-0.56056	-1.56476
0.40000	-2.26448	-1.12111	-1.14337
0.60000	-2.42595	-1.68167	-0.74428
0.80000	-2.62459	-2.24222	-0.38237
1.00000	-2.87559	-2.80278	-0.07281
1.50000	-3.68926	-4.20416	0.51490
2.00000	-4.60555	-5.60555	1.00000
2.50000	-5.54809	-7.00694	-1.45885
3.00000	-6.50000	-8.40833	1.90833
4.00000	-8.41480	-11.21110	2.79630

Table 3: The energy of one hole ($\in_h$) as a function of J for 8 sites

J	$\in_t$	$\in_N$	$\in_h$
0.00000	-2.00000	0.000000	-2.000000
0.01000	-2.01073	-0.036511	-1.974219
0.02000	-2.02151	-0.073022	-1.948488
0.05000	-2.05407	-0.182555	-1.871515
0.10000	-2.10919	-0.365109	-1.744081
0.20000	-2.22278	-0.730219	-1.492561
0.40000	-2.46642	-1.460440	-1.005980
0.60000	-2.73957	-2.190660	-0.548910
0.80000	-3.04830	-2.920870	-0.127430
1.00000	-3.38765	-3.651090	0.263440
1.50000	-4.30462	-5.478840	1.174220
2.00000	-5.25684	-7.302190	2.045350
2.50000	-6.65290	-9.127730	2.474830
3.00000	-8.05863	-10.953300	2.894670
4.0000	-10.8808	-14.604400	3.723600

Table 4: The energy of one hole ($\in_h$) as a function of J_z for 4 sites (The Ising chain)

J_z	$\in_t$	$\in_N$	$\in_h$
0.00000	-2.00000	0.00000	-2.00000
0.01000	-2.00167	-0.01000	-1.99167
0.02000	-2.00334	-0.02000	-1.98334
0.05000	-2.00838	-0.05000	-1.95838
0.10000	-2.01685	-0.10000	-1.91685
0.20000	-2.03408	-0.20000	-1.83408
0.40000	-2.06969	-0.40000	-1.66969
0.60000	-2.10688	-0.60000	-1.50688
0.80000	-2.14568	-0.80000	-1.34568
1.00000	-2.18614	-1.00000	-1.18614
1.50000	-2.29473	-1.50000	-0.79473
2.00000	-2.41421	-2.00000	-0.41421
2.50000	-2.54473	-2.50000	-0.04473
3.00000	-2.68614	-3.00000	0.31386
4.00000	-3.00000	-4.00000	1.00000

Table 5: The energy of one hole ($\in_h$) as a function of J_z for six sites (The Ising chain)

J	$\in_t$	$\in_N$	$\in_h$
0.00000	-2.00000	0.00000	-2.00000
0.01000	-2.00600	-0.01500	-1.99100
0.02000	-2.01201	-0.03000	-1.98201
0.05000	-2.03005	-0.07500	-1.95505
0.10000	-2.06020	-0.15000	-1.91020
0.20000	-2.12082	-0.30000	-1.82082
0.40000	-2.24338	-0.60000	-1.64338
0.60000	-2.36782	-0.90000	-1.46782
0.80000	-2.49428	-1.20000	-1.29428
1.00000	-2.62291	-1.50000	-1.12291
1.50000	-2.95479	-2.25000	-0.70479
2.00000	-3.30278	-3.00000	-0.30278
2.50000	-3.66785	-3.75000	0.08215
3.00000	-4.04998	-4.50000	0.45002
4.00000	-4.86081	-6.00000	1.13919

Table 6: The energy of one hole ($\in_h$) as a function of J_z for eight sites (The Ising chain)

J	$\in_t$	$\in_N$	$\in_h$
0.00000	-2.00000	0.00000	-2.00000
0.01000	-2.01072	-0.02000	-1.99072
0.02000	-2.02144	-0.04000	-1.98144
0.05000	-2.05362	-0.10000	-1.95362
0.10000	-2.10735	-0.20000	-1.90735
0.20000	-2.21514	-0.40000	-1.81514
0.40000	-2.43213	-0.80000	-1.63213
0.60000	-2.65121	-1.20000	-1.45121
0.80000	-2.87264	-1.60000	-1.27264
1.00000	-3.09665	-2.00000	-1.09665
1.50000	-3.66958	-3.00000	-0.66958
2.00000	-4.26308	-4.00000	-0.26308
2.50000	-4.87808	-5.00000	0.12192
3.00000	-5.51338	-6.00000	0.48662
4.0000	-6.83424	-8.00000	1.16576

6.0 Conclusion

We have calculated the energy of a single hole in one dimensional quantum antiferromagnet, using the exact diagonalization method. The result shows that the spin flip term in the $t-J$ model plays a dominant role in the coherent propagation of the

hole. Here, in this work, it is found that the energy expended by the hole decreases with the size of the system. Hence, the single hole in the more robust $t-J$ model does not suffer from any confinement, as the length of the chains is increased. This is in sharp contrast to the motion of a single hole in the $t-J_z$ model (Ising limit), where the hole suffered from weak confinement, arising from weak linear potential that grows with the length of the chain. This obvious difference in the dynamics of the hole between $t-J$ and $t-J_z$ models in 1D is due to the presence of the spin flip term in the $t-J$ model, which helps to relax a pair of overturned spin created by hole motion. Hence, the weak string excitation, which grows with N, observed in 1D $t-J_z$ model is completely absence in 1D $t-J$. Therefore, while spin-charge separation becomes evident in the thermodynamic limit (large N) for the Ising chains, it can easily be observed in finite chains (small N) for the Heisenberg chains. This deconfinement of hole in one dimensional quantum antiferromagnet lends credence to both theoretical and experimental reports of spin charge separation in one dimensional Mott Insulator [16, 17, 18, and 23].

It is important to note that the dynamics of a single hole in two dimensional Mott insulators is not a very rosy one. Here, the hole motion in the antiferromagnet (AF) gives rise to the creation of spin fluctuations, which are defects in the underlying magnetic background [24, 25]. These defects lie on chains formed on paths along which the hole has moved. The length of such chains is in principle proportional to the increase in the exchange energy (J). Thus, the chains act on the hole as strings. The hole which can retrace the path to its starting point behaves as a particle in a linear rising potential well, with the center on the initial position of the hole. A Hamiltonian for the problem of the hole in the potential well originating with the string effect has eigenstates with well defined energies. These states are related with a well defined modification of the AF background, thus they can be interpreted as AF spin polarons. Furthermore, in the limit of $J/t \ll 1$, the spin-relaxation time is much longer than the characteristic time for hoping. As a result, the rate at which the spins are being flipped by the hole is faster than the rate at which they are being repaired by the spin flip term in the $t-J$ model. This is the obvious reason for the present of string excitations in both the two dimensional Ising and Heisenberg spin chains.

7.0 References

[1] Bednorz J. G. and Müller K. A. (1986). Possible high Tc superconductivity in the Ba−La−Cu−O system. Z. Physik, B 64, 189–193.

[2] Birgeneau R.J. and Shirane G. (1989). In Physics Properties of High Temperature Superconductors, Vol.1, edited by D.M. Ginsberg (World Scientific, Singapore) p.151.

[3] Brinkmann W.F. and Rice T.M. (1970). Single-particle excitations in Magnetic Insulators. Phy. Rev. B2, 1324-1336.

[4] Manuosakis E. (2007). String excitations of a hole in a quantum antiferromagnet and photoelectron Spectroscopy. Phys. Lett. A 362, 86-89.

[5] Shraiman B. I. and Siggia. E. D. (1988). Two-Particle Excitations in Antiferromagnetic Insulators. Phys. Rev., B60, 740-743.

[6] Ronning F., Shen K. M., Armitage N. P., Damascelli A., Lu D.H., Shen Z.-X., Miller L. L. and. Kim C.(2005). Anomalous high-energy dispersion in angle-resolved photoemission spectra from the insulating cuprate Ca2CuO2Cl2 . Phys. Rev.B 71, 094518-1—5.

[7] Doiron-Leyraud N., Proust C., LeBoeuf D., Levallois J., Bonnemaison J.-B., Liang R., Bonn D.A., Hardy W.N., Taillefer L. (2007). Quantum oscillations and the Fermi surface in an underdoped high-Tc superconductor. Nature 447, 565-568.

[8] Prelovšek P., Sega I. and Bonča J. (1990). Cummulant-expansion study of holes in quantum antiferromagnet. Phys. Rev. B42, 10706-10713.

[9] Singh R. J. and Khan S. (2014). Hole-Pair Formation in Cuprate Superconductors despite Antiferromagnetic Fluctuations. World Journal of Condensed Matter Physics, 4, 141-152.

[10] Trugman S.A. (1988). Interaction of holes in a Hubbard antiferromagnet and high-temperature superconductivity. Phys. Phys. Rev. B37, 1597-1603.

[11] Lin H. Q., Hirsch J. E. and Scalapino D. J. (1988). Pairing in the two-dimensional Hubbard model: An exact diagonalization study. Phys. Rev. B 37, 7359 -7367.

[12] Guan X. W., Batchelor M. T. and Lee C. (2013). Fermi gases in one dimension: From Bethe ansatz to experiments. Rev. Mod. Phys. 85, 1633-1691.

[13] Raczkows M., Assaad F. F. and Lode P. (2015). Spin and charge dynamics of a quasi-one-dimensional antiferromagnetic metal. Phys. Rev. B 91, 045137-1—14.

[14] Brunner M., Assaad F. F. and Muramatsu A. (2000). Single hole dynamics in the one dimensional $t-J$ model. Eur. Phys. J. B 16, 209-212.

[15] Matsueda H., Tohyama T. and Maekawa S. (2006). Electron-phonon coupling and spin-charge separation in one-dimensional Mott insulators Phys. RevB.74, 241103-1—4.

[16] Kim C., Spin–charge separation in 1D Mott-insulator and related systems. JESRP, Vol.117-118, (2001) 503-515.

[17] Kidd T. E., Valla T., Johnson P. D., Kim K. W., Gu G. D. and Homes C. C. (2008). Doping of a one-dimensional Mott insulator: Photoemission and optical studies of Sr2CuO3+δ. Phys. Rev. B 77, 054503-1—7.

[18] Fujisawa H., T. Yokoya and Takahashi T. (1999). Angle-resolved photoemission study of Sr2CuO3. Phys. Rev. B 59, 7358-7362.

[19] Schlappa J., Wohlfeld K., Zhou K. J, Mourigal M., Haverkort M. W., Strocov V. N., Hozoi L., Monney C., Nishimoto S., Singh S., Revcolevschi A., Caux J.-S., L. Patthey, Rønnow H. M., van den Brink J. and Schmitt T. (2012). Spin-orbital separation in the quasi-one-dimensional Mott insulator Sr2CuO3, Nature 485, 82-85.

[20] Moreno, A. Muramatsu and J. M. P. Carmelo (2013). Charge and spin fractionalization beyond the Luttinger-liquid paradigm. Phys. Rev. B 87, 075101-1—7.

[21] Hubbard J. (1963). Electron correlations in narrow energy bands. Proc. Roy. Soc. London Ser.A276, 238-257.

[22] Ehika S. and Idiodi J.O.A. (unpublished). Possibility of hole confinement in the weak coupling regime of finite one dimensional Ising antiferromagnets and the emergence of spin-charge separation in the bulk limit.

[23] Sorella S. and Parola A. (1992). Spin-charge decoupling and the greens-function of one-dimensional Mott insulators. Phys. Rev. B45, 13156-13159.

[24] Ehika S. and Idiodi J.O.A. (2012). The dynamics of a hole in two dimensional Mott insulators. Journal of NAMP Vol. 21, 1-10.

[25] Dagotto E. (1994). Correlated electrons in high-temperature superconductors. Rev. Mod. Phys., 66, 763-840.